Test of the mechanotactile hypothesis: neuromast morphology and response dynamics of mechanosensory lateral line primary afferents in the stingray

Karen P. Maruska* and Timothy C. Tricas

Department of Zoology and Hawai'i Institute of Marine Biology, University of Hawai'i at Manoa, 2538 The Mall, Honolulu, HI 96822, USA

*Author for correspondence (e-mail: maruska@hawaii.edu)

Summary

The mechanotactile hypothesis proposes that ventral non-pored lateral line canals in the stingray function to facilitate localization of prey that contact the skin during benthic feeding. This study used comparative neurophysiological and morphological techniques to test whether ventral non-pored canals encode the velocity of skin movements, and show other adaptations that may enhance detection of tactile stimuli from their prey. Resting discharge rate of lateral line primary afferent neurons was lower among units from ventral than dorsal canal groups. The ventral non-pored canals had a higher proportion of silent units (31%) than either ventral (3%) or dorsal (13%) pored canals, thus may have an enhanced potential for detection of phasic contact with prey. Primary afferents from pored canals showed response characteristics consistent with acceleration detectors, with best frequencies of 20–30 Hz. In contrast, units from non-pored canals responded to tactile skin depression velocities of 30–630 μm s^{-1} from 1–20 Hz, and encoded the velocity of canal fluid induced by skin movement with best frequencies of $\leqslant$10 Hz. Sensitivity of non-pored canals to direct skin depression velocity was 2–10 times greater than to hydrodynamic dipole stimulation near the skin. No morphological specialization of hair cell orientation was found among pored and non-pored canals. These low frequency, tactile response properties support the hypothesis that the stingray's non-pored ventral lateral line functions as a mechanotactile receptor subsystem used to guide small benthic invertebrates to the ventrally positioned mouth.

Key words: canal, elasmobranch, frequency response, hair cell, neuromast, lateral line, stingray, *Dasyatis sabina*.

Introduction

The mechanosensory lateral line system of fishes is best known as a detector of hydrodynamic flow across the body surface (for a review, see Coombs and Montgomery, 1999). Peripheral lateral line gross morphology and neuromast position determine the hydrodynamic features that are encoded at the hair cell – primary afferent neuron level. The lateral line system of elasmobranchs (sharks, skates and rays) consists of superficial neuromasts (pit organs) and two morphological classes of sub-epidermal canals (see review by Maruska, 2001). Superficial neuromasts are single units positioned on the skin in shallow grooves (batoids) or between modified scales (sharks), are in direct contact with external hydrodynamic flow fields near the body, and encode water velocity to mediate behaviors such as rheotaxis (Montgomery et al., 1997; Peach, 2001). In contrast, lateral line canals occur beneath the skin surface, and have a continuous sensory epithelium within a fluid-filled canal. The kinocilium/stereocilia axis of canal hair cells typically shows a strong polarity along the longitudinal axis of the canal that maximizes neural sensitivity to canal fluid motion (see Flock, 1965; Roberts, 1969). Elasmobranch canals are further distinguished by either the presence of skin pores

that permit direct contact with the surrounding water (i.e. pored canals), or an absence of skin pores that eliminates direct contact of canal fluid with the external environment (i.e. non-pored canals) (Ewart and Mitchell, 1892; Johnson, 1917; Boord and Campbell, 1977; Chu and Wen, 1979). The motion of fluid in pored canals of teleost fishes is induced by hydrodynamic pressure differences at the skin pores. Thus pored canal neuromasts encode the acceleration of external water flow near the skin, and mediate behaviors such as schooling, hydrodynamic imaging and prey detection (for a review, see Coombs and Montgomery, 1999). However, with the exception of prey detection (Montgomery and Skipworth, 1997), such functions for the pored lateral line have yet to be experimentally demonstrated for elasmobranch fishes and the neurophysiological response properties are poorly known.

The extensive non-pored canals of sharks and batoids are located primarily on the ventral body surface, the rostrum and around the mouth (Chu and Wen, 1979; Maruska, 2001). The absence of skin pores indicates that pressure differences caused by localized weak hydrodynamic flow will not directly produce canal fluid motion, as occurs in pored canal systems. Although

the non-pored system of batoids was used to model the sensitivity of lateral line neuromasts to fluid velocity (Sand, 1937), the response properties of the non-pored canal system in relation to natural behaviors such as prey localization are unknown.

The mechanotactile hypothesis was proposed to explain one function for non-pored canals in elasmobranch fishes (Maruska and Tricas, 1998). This hypothesis states that the non-pored canals on the ventral surface of the stingray function as tactile receptors that facilitate localization and capture of small benthic invertebrate prey. The mechanotactile hypothesis generates several testable, though not mutually exclusive, predictions about the stimulus encoding properties of this system. First, direct coupling of the skin and canal fluid should result in sensitivity to the velocity of skin movement. Thus, primary afferents that innervate neuromasts in non-pored canals should show characteristics more consistent with detectors of the velocity rather than the acceleration of skin depression. Second, without direct connection to the environment, non-pored canals should have a lower sensitivity to dipole water motion compared to direct tactile stimulation. Third, if non-pored canals represent a specialized tactile system, they may show neurophysiological adaptations that enhance the discrimination of prey such as silent units to facilitate detection of phasic stimuli. In addition, they should show greater tactile sensitivity than the general cutaneous somatosensory system that has a displacement threshold of about $20\,\mu m$ (Murray, 1961). Fourth, if non-pored canals function as touch receptors to detect transient skin movements adjacent to the canal, then non-pored canals may have a greater proportion of hair cells oriented orthogonal to the canal axis compared to pored canals. These non-axial hair cell orientations shown in some chondrichthyan fishes (Roberts, 1969; Roberts and Ryan, 1971; Ekstrom von Lubitz, 1981; Maruska, 2001) could encode lateral cupular deflections to expand the tactile receptive field to include areas adjacent to the canal.

This study tests these predictions of the mechanotactile hypothesis by determination of the frequency–response properties of primary afferent neurons that innervate neuromasts in pored and non-pored canals in the stingray. In addition, we assess hair cell orientations among canal groups to test the prediction that non-pored canals have a greater proportion of hair cells oriented orthogonal to the canal axis compared to pored canals. Our results provide neurophysiological support for the mechanotactile hypothesis and are interpreted in relation to the natural behavior and ecology of this elasmobranch fish.

Materials and methods
Neurophysiology

Adult male and female Atlantic stingrays *Dasyatis sabina* Lesueur were collected with a dip net from the Banana River, Florida, USA. Stingrays were transported back to the laboratory and used for neurophysiology experiments within 2 h of capture. Neurophysiology was performed on a total of 14 stingrays: 11 male (disk width = 22.5–26.0 cm) and three female (disk width = 27.0–29.0 cm) rays (8 dorsal preparation, 6 ventral preparation). Experimental procedures followed guidelines for the care and use of animals approved by the Institutional Animal Care and Use Committee at Florida Institute of Technology. Experimental animals were deeply anesthetized with 0.02% tricaine methanesulfonate (MS222) and then immobilized by intramuscular injections of pancuronium bromide ($\sim$0.3 mg kg^{-1} body mass). Rays were clamped on an acrylic stage in an experimental tank (61 cm long $\times$ 41 cm wide $\times$ 15 cm deep) supported by a vibration isolation table. Stingrays were ventilated by a continuous flow of fresh seawater (22–23°C) that did not contain MS222 throughout the experiment because of the negative effects of this anesthetic on lateral line afferent activity (Späth and Schweickert, 1977). A portion of the anterior lateral line nerve, which contains mechanosensory lateral line afferent and efferent neurons, was surgically exposed either posterior to the spiracle (dorsal preparation), or lateral to the first gill slit (ventral preparation). The perineurium was separated on a small section of the nerve fassicle to facilitate single unit recordings. Neurophysiological recordings were focused on primary afferents that innervate neuromasts in the dorsal pored (Dp), ventral pored (Vp) and ventral non-pored (Vnp) sections of the hyomandibular canal (HYO), which covers a large portion of the pectoral fins on both the dorsal and ventral surface (Fig. 1). The water level within the tank was kept approximately 1 cm below the surgical opening so that all hyomandibular canal pores on the pectoral fins were submerged.

Extracellular single unit recording experiments used glass microelectrodes (15–50 MΩ, 4 mol l^{-1} NaCl) visually guided under a microscope to the nerve surface. Lateral line primary afferents were distinguished from electrosensory afferents by their phasic response to a water movement stimulus delivered to the tank with a pipette. Neuromast locations were identified by probing the skin with a small water jet or probe. Dipole hydrodynamic stimuli were produced by a plastic sphere attached to an 18-guage stainless steel shaft and sinusoidally driven by a function generator and minishaker. Sphere diameter was either 6 mm (ventral recordings) or 9 mm (dorsal recordings), both of which are within the size range of natural invertebrate prey (Cook, 1994). The sphere was positioned with an *XYZ* slider system and the dipole axis fixed at a 45° angle to the skin surface 2–3 mm above the skin for pored canals, or in direct contact with the skin above the canal for non-pored canals. Receptive fields for Dp and Vp canals were located over pores on the pectoral fins, while the receptive field for Vnp canals was centered over the sub-epidermal canal located along the ventral midline. To test the prediction that non-pored canals are most sensitive to touch, the response of primary afferents from non-pored canals to direct tactile stimulation was compared to that of a hydrodynamic flow source 2–3 mm above the canal.

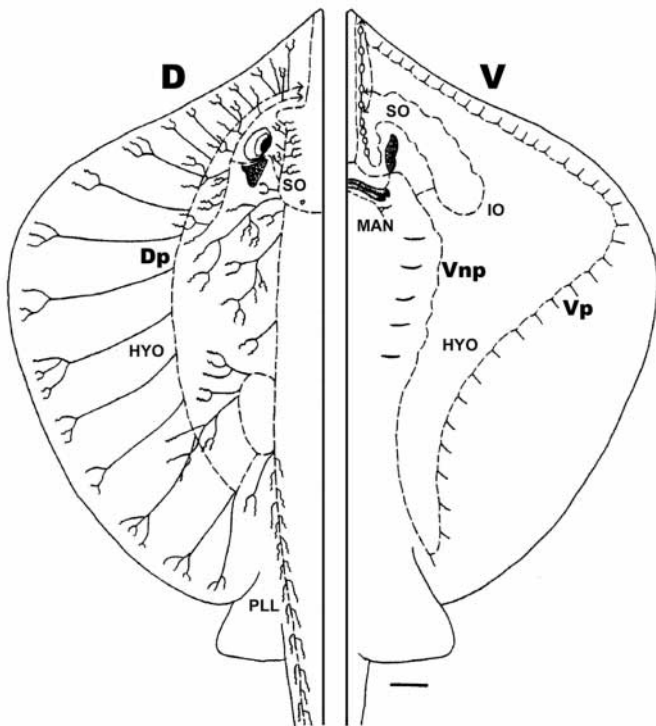Displacement amplitude of the sphere was controlled by a

Fig. 1. The lateral line canal system on the dorsal (D) and ventral (V) surface of the Atlantic stingray, *Dasyatis sabina*. Broken lines indicate sections of canal that contain innervated neuromasts, while solid lines represent neuromast-free tubules that terminate in pores. Neurophysiology recordings were made from primary afferent neurons in the anterior lateral line nerve that innervate neuromasts in the dorsal pored (Dp), ventral pored (Vp), and ventral non-pored (Vnp) hyomandibular canals (HYO). Note that the dorsal HYO contains numerous lateral tubules that branch to terminate in pores, while the ventral hyomandibular canal contains a lateral pored section and a medial non-pored section along the midline. IO, infraorbital canal; MAN, mandibular canal; PLL, posterior lateral line canal; SO, supraorbital canal. Scale bar, 1 cm. Modified from Maruska and Tricas (1998).

function generator and a servocontrol feedback system in order to maintain constant source peak-to-peak (PTP) stimulus amplitudes. Peak sphere displacement at each stimulus amplitude and frequency was calibrated under a microscope and showed a linear relationship over this stimulus range. The amplitude of the water displacement at the skin surface (d) was estimated by $d=U(R/D)^3$, where U is the amplitude of sphere displacement, R is the radius of the sphere, and D is the distance between the center of the sphere and the skin (Kroese and Schellart, 1992). Estimated water displacement amplitudes at the skin surface (d) ranged from approximately 0.1–270 µm (for 6 and 9 mm spheres). This estimation method is limited because it does not take into account the influence of the nearby skin and effect of the boundary layer. However, boundary layer effects were probably not significant in this study because all neuromasts were located inside canals and not on the skin surface (see Kroese and Schellart, 1992). Stimulus frequencies

ranged from 1 to 220 Hz with a minimum of 3 s of rest activity between each stimulation trial. For each individual afferent, the amplitude of sphere displacement remained constant as frequency was changed. Frequency sweeps began at 30 Hz, followed by testing of higher frequencies up to 220 Hz and then a return to test frequencies <30 Hz. For each stimulus frequency a minimum of 500 spikes were collected for peristimulus periods. Neural activity was monitored visually on an oscilloscope and acoustically on a loud speaker. Analog neural discharge signals were amplified, filtered at 300–3000 Hz, and stored on tape.

The tactile receptive field for non-pored canal primary afferents was estimated by lightly probing the skin with an 800 µm diameter sphere attached to a thin insect pin shaft at a frequency of ~1 Hz above and adjacent to the canal. The distance between the points of maximum neural excitation (directly over the canal) and no response (neuron returns to spontaneous rate or silent), S, was measured to the nearest mm orthogonal to the canal axis. Receptive field area was then calculated as $(2S)^2$. This is a conservative estimate of receptive field area because the response distance directly along the canal axis was on average at least twice as great as the response distance S that was orthogonal to the canal axis.

Analyses of single unit responses were conducted off-line. Analog spikes were discriminated and converted to digital event files *via* a Cambridge Electronic Design 1401 and Spike 2 software (Cambridge, UK). Interspike interval (ISI) histograms of resting discharges were generated from 500 consecutive spikes compiled in 2 ms bins. Resting discharge ISI histograms were used to classify units as regular (unimodal with near identical median and mode) or irregular (Poisson-like distribution). Silent afferents showed no spontaneous activity and discharged only when stimulated. Resting discharge variability was expressed as the coefficient of variation (CV), which is the dimensionless ratio of standard deviation (S.D.) to mean ISI. A regular unit was defined by a unimodal distribution and CV<0.40, and an irregular unit by a distribution skewed to the right and CV>0.40. Resting discharge characteristics that were not normally distributed were compared among canal subsystems by non-parametric Kruskal–Wallis one-way analysis of variance (ANOVA) on ranks and differences determined by Dunn's multiple comparisons test. Data that passed normality and equal variance tests were compared with a one-way ANOVA and subsequent Tukey's test.

To determine whether the neural responses were linear, several afferents were tested at multiple stimulus amplitudes for each frequency. Linearity was examined by plotting response amplitude (peak discharge – average resting rate) as a function of stimulus amplitude. These preliminary experiments confirmed that the neural responses are linear relative to stimulus amplitude, as found in other lateral line systems (e.g. Kroese et al., 1978; Münz, 1985; see Results below).

Neural sensitivity, frequency and phase responses of units were determined by construction of period histograms (128

bins) and period analyses. A Fourier transformation of the period histogram was used to generate coefficients for mean resting rate (DC), peak discharge rate, and the phase relationship between the peak unit response and the stimulus peak. Neural sensitivity for individual units was calculated as [(peak discharge rate − DC)/stimulus amplitude]. In order to compare neural responses among units, sensitivity was converted to relative neural gain (dB) calculated as $20 \times \log$(neural sensitivity).

Best frequency (BF) of each neuron was defined as the frequency that evoked the greatest increase in the number of spikes above mean resting rate (peak discharge rate − DC). Data used to generate frequency–response curves were normalized by assigning a value of 0 dB to BF in order to control for absolute differences in sensitivities among afferents. d at the skin surface was estimated as described above and converted to velocity (u) and acceleration (a) values with the relationships $u=2\pi f d$ and $a=4\pi^2 f^2 d$, where f is the sphere vibration frequency and d is estimated peak-to-peak or peak displacement at the skin surface (Coombs and Janssen, 1990a). Neural sensitivity for units from pored canals was estimated from PTP stimulus and response, whereas peak stimulus and response values were used for units from non-pored canals because the sphere was in contact with the skin for only half of the sinusoidal stimulus cycle. To illustrate the difference in relative sensitivity between tactile and hydrodynamic stimuli, afferent responses to tactile stimuli were normalized relative to responses to hydrodynamic flow. Neural sensitivity to hydrodynamic flow was assigned a gain value of 0 dB, and relative neural gain (dB) to tactile stimuli calculated as $20 \times \log$(tactile neural sensitivity/hydrodynamic neural sensitivity). The phase relation between the stimulus and neural discharge response was expressed as the difference in arc degrees between the peak discharge rate and peak stimulus amplitude.

Hair cell orientations

Hair cell sensitivity to fluid flow in lateral line canals is dependent upon the orientation of kinocilia and stereocilia relative to the longitudinal axis of the canal. Hair cell polarities were determined to test the prediction that a greater number of hair cells are oriented orthogonal to the longitudinal canal axis in non-pored canals compared to pored canals. Adult stingrays were euthanized with an overdose of MS222, the epidermis removed, canals opened to expose the neuromasts, and cupulae mechanically dislodged from neuromasts by a gentle water jet. Approximately 2–5 neuromasts were removed from Dp, Vp and Vnp hyomandibular canals in each animal, fixed for 1–2 h in 2% glutaraldehyde in Millonig's buffer, and soaked in Millonig's buffer overnight. Tissue was then rinsed in 0.05 mol l^{-1} phosphate buffer (PB), postfixed in 1% osmium tetroxide, rinsed again in PB and dehydrated in an ethanol series (50–100%). Neuromasts were dried in an LADD (Burlington, VT, USA) critical point dryer with carbon dioxide as a transitional fluid and sputter-coated with gold–palladium alloy. Samples were viewed on a Hitachi S-2700 scanning electron microscope (SEM) at an accelerating voltage of 8–10 kV and images recorded on VHS tape for analysis.

Individual hair cell orientation was determined by the semicircular angular deviation (from 0–180°) from the axis of maximum excitation of the hair cell (towards the kinocilium) to the longitudinal axis of the neuromast (canal axis). Orientations were measured for 10 randomly selected hair cells from several neuromasts in each of the three canals (Dp, Vp and Vnp) in each animal. Hair cell orientation data failed tests of normality and could not be normalized by transformation. Thus, the non-parametric Kruskal–Wallis one-way ANOVA on ranks was used to test whether hair cell orientations differed among neuromasts located in different canal subsystems.

Results

Resting discharge activity

Primary afferents recorded in this study innervated neuromasts located within the main hyomandibular canal on the disk from the rostrum to the caudal edge of the pectoral fin on the dorsal surface, and the hyomandibular loop from the first gill slit to the caudal edge of the pectoral fin on the ventral surface (see Fig. 1). Resting discharge activity was recorded from a total of 136 primary afferent neurons in 14 stingrays and spontaneous rates ranged from 0 (silent) to 59.8 spikes s^{-1}. Neurons with regular, irregular and silent discharge patterns were recorded from all canal types (Table 1). The most commonly encountered units overall had irregular discharge

Table 1. *Spontaneous discharge characteristics of lateral line primary afferent neurons that innervate neuromasts in the dorsal pored (Dp), ventral pored (Vp) and ventral non-pored (Vnp) hyomandibular canals of the stingray*

	Dp (72)			Vp (16)			Vnp (48)		
	R (30)	I (40)	S (2)	R (8)	I (6)	S (2)	R (18)	I (15)	S (15)
Units (%)	41.7	55.6	2.7	50	37.5	12.5	37.5	31.25	31.25
Resting discharge (spikes s^{-1})	16.3, 21.8, 25.3	9.7, 17.2, 28.3	NA	11.6, 17.1, 21	4.9, 9.6, 11.5	NA	6, 9.9, 15.9	5.4, 16.2, 22.2	NA
Mean ± S.E.M.	20.5±1.1	20.7±2.3	NA	16.7±2.6	8.9±2.1	NA	11.4±1.6	16.3±3.3	NA

R, regular; I, irregular; S, silent; NA, not applicable. Resting discharge data are expressed as 25%, median, 75% quartiles (top line), and mean ± S.E.M. (bottom line). The total number of primary afferents sampled from each discharge class within each canal subsystem is indicated in parentheses.

patterns (45%), followed by regular (41%), and silent (14%). However, when percentages were examined by canal subsystem, Vp and Vnp canals both had a higher percentage of regular units while Dp canals showed more irregular units (Table 1). Primary afferents with bursting spontaneous activities or bimodal ISI distributions (Münz, 1985; Tricas and Highstein, 1991) were not observed. Fig. 2 illustrates the variation in spike distribution of regular and irregular discharging units for 12 representative neurons. Both fast (ISI <80 ms) and slow (ISI >100 ms) regular discharging units were isolated, with a high percentage of slow firing units innervating neuromasts in the Vnp canal (Figs 2, 3). Irregular discharging afferents had ISI distributions skewed to the right and CV>0.40 (Fig. 2). Silent afferents represented about 31% of total units

in Vnp canals, but were much less common in Vp (12.5%) and Dp (2.7%) canals (Table 1; Fig. 3).

There were no differences in resting discharge activity, ISI or CV among the total population of afferents that innervate Dp and Vp canals (Kruskal–Wallis one-way ANOVA on ranks, $P>0.05$). However, resting discharge characteristics of lateral line primary afferents are further categorized into regular, irregular and silent units within each canal type and are summarized in Table 1. The plots in Fig. 4 show a clear separation between regular and irregular afferents among canal types with respect to CV, but some overlap and greater variability with respect to ISI. Primary afferents classified as regular differed only between Dp and Vnp canals in CV (one-way ANOVA, Tukey's test, $P<0.05$), resting discharge activity
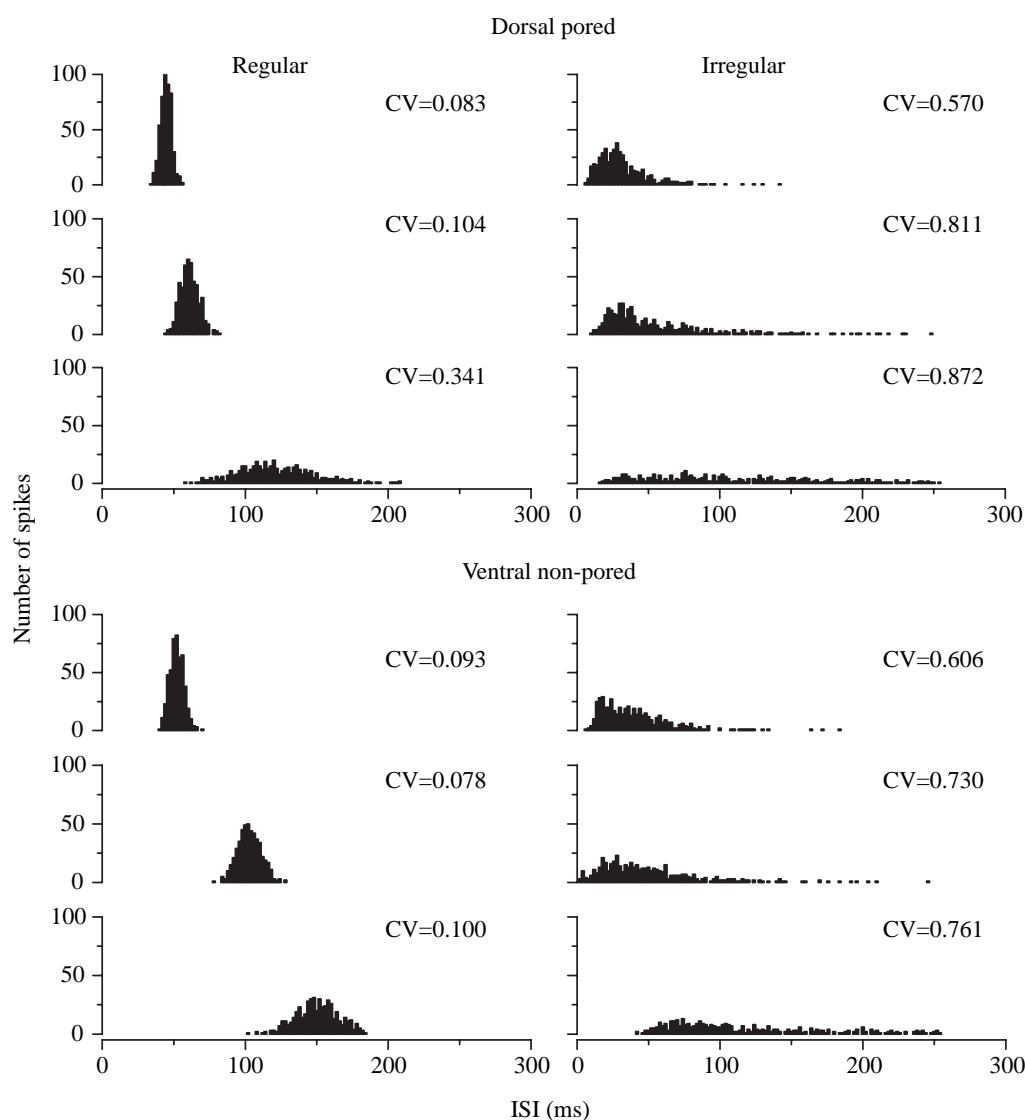

Fig. 2. Resting discharge patterns for individual primary afferent neurons that innervate dorsal and ventral hyomandibular lateral line neuromasts in the Atlantic stingray, *Dasyatis sabina*. Interspike interval (ISI) histograms shown for individual neurons are representative of those recorded from primary afferents in all canal subsystems. Irregular resting discharge patterns were most common (45% of all units) and ISI distributions were similar among dorsal and ventral primary afferents. Regular firing afferents from ventral non-pored canals had slower discharge activity (greater ISI) than those from dorsal pored canals. Histograms were calculated from 500 consecutive spikes and compiled in 2 ms bins. Discharge variability is expressed as the coefficient of variation (CV), which is the dimensionless ratio of s.d. to mean interspike interval.

(one-way ANOVA, Tukey's test, $P<0.05$), and interspike intervals (Kruskal–Wallis one-way ANOVA on ranks, Dunn's test, $P<0.05$). Thus, regular primary afferents in Dp canals had a greater CV and resting discharge activity, but lower ISI compared to Vnp regular afferents (Fig. 4). In contrast, primary afferents classified as irregular did not differ with respect to these characteristics (Kruskal–Wallis one-way ANOVA on ranks, $P>0.05$).

Frequency–response

Frequency–response characteristics were determined for a total of 77 lateral line primary afferent neurons (Dp=40, Vnp=28 and Vp=9) in 14 stingrays. Sinusoidal stimulation of the lateral line system produced modulation of primary afferent spontaneous activity, and evoked discharges from silent units. Recordings were made at stimulus amplitudes where there was a linear relationship between peak neural response and stimulus intensity. The amplitude of the response was proportional to the amplitude of the stimulus across the range of frequencies used (Fig. 5). The gain and phase of the response of individual afferents was independent of the stimulus amplitude, and confirms linearity for this system.

When neural responses of units from Dp canals were plotted
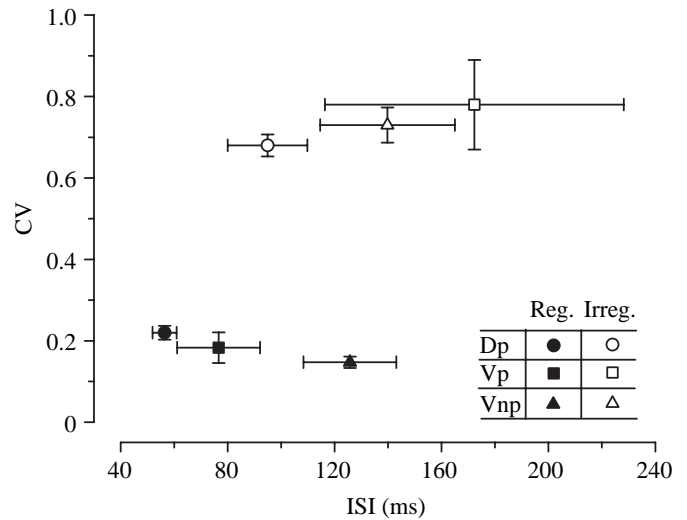
Fig. 4. Relationship between mean interspike interval (ISI) and coefficient of variation (CV) for regular and irregular primary afferent neurons from dorsal pored (Dp), ventral pored (Vp) and ventral non-pored (Vnp) canals in the Atlantic stingray, *Dasyatis sabina*. Primary afferents with regular discharge activity (Reg; closed symbols) have lower CV values than irregular units (Irreg; open symbols) for all canal types. ISI values differ between regular and irregular units for Dp and Vp, but not Vnp primary afferents. Further, regular Dp afferents have higher CV and lower ISI values than regular Vnp afferents. Data are plotted as mean ± S.E.M.
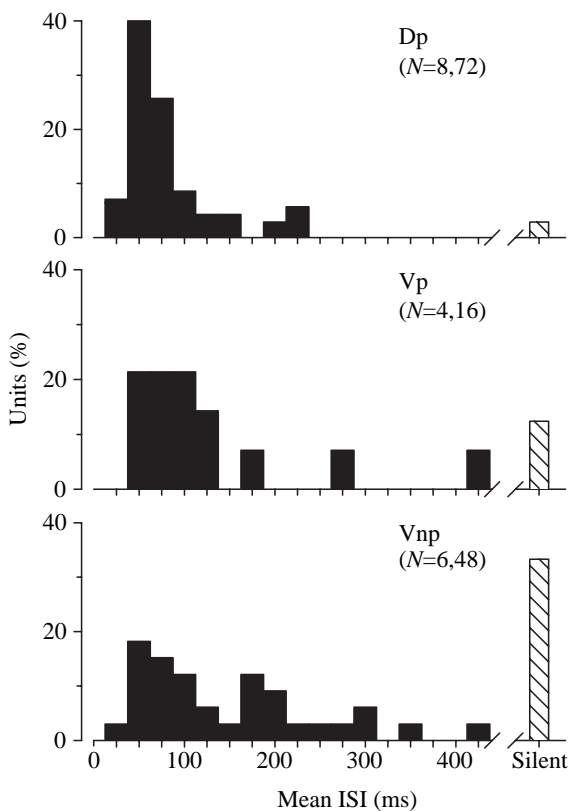

Fig. 3. Interspike interval (ISI) frequency histograms of primary afferent neurons that innervate dorsal pored (Dp), ventral pored (Vp) and ventral non-pored (Vnp) hyomandibular canal neuromasts in the Atlantic stingray, *Dasyatis sabina*. Primary afferents that innervate Vnp canals show slower, more variable resting rates than do units from Dp and Vp canals. Also, approximately one-third of units in Vnp canals had no resting discharge (i.e. were silent). These features of the non-pored lateral line primary afferents are consistent with the idea of enhanced detection of transient or phasic stimuli produced by prey. Sample sizes (N) show the number of animals, number of primary afferents sampled.
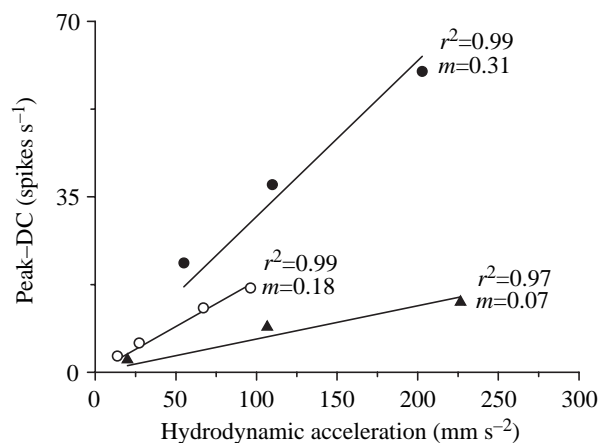

Fig. 5. Relationship between neural response at best frequency and stimulus intensity for three representative primary afferent neurons from the dorsal pored hyomandibular canal of the Atlantic stingray, *Dasyatis sabina*. Relative neural gain varies among these units, but neural discharge (peak–DC) increases as a linear function of stimulus intensity (re: hydrodynamic acceleration estimated at the skin surface) for all three. *m*, slope.

as a function of water velocity, they showed band-pass characteristics with a –6dB bandwidth of 20–90 Hz (Fig. 6Ai). Neural responses of afferents from Vp canals showed low-pass characteristics to hydrodynamic stimuli re: velocity with a response above –6dB maintained <70 Hz (Fig. 6Bi). When the skin was stimulated above Vnp canals, primary afferents from Vnp canals had a flat low-pass characteristic <30 Hz re: velocity with a measured best frequency of 8.6±1.3 Hz (mean ± S.E.M.; Fig. 6Ci). Relative to acceleration, primary afferents from Dp and Vp canals showed a flat frequency response to hydrodynamic stimuli re: acceleration below 30 Hz (Fig. 6Aii,Bii). Thus, primary afferents from Dp canals show frequency response characteristics consistent with acceleration detectors as per Coombs and Janssen (1989). The response of primary afferents from Vp canals showed properties of both an acceleration and a velocity detector, which may be partially due to the large variation and small sample size of this group

of afferents. In contrast, primary afferents from Vnp canals showed low-pass characteristics to tactile stimuli re: acceleration with a 6 dB drop in neural gain achieved by 5 Hz (Fig. 6Cii). Further, primary afferents from Vnp canals show frequency-independent response characteristics to tactile stimuli re: velocity below 30 Hz, which is consistent with velocity detectors (Fig. 6Ci). Although frequency–response differences were identified among canal subsystems, there was no obvious relationship between neuromast location on the body and best frequency of primary afferents.

The low frequency slope of the frequency–response curve relative to displacement for afferents that innervate Dp canal neuromasts (x=37.3±7.8 dB decade^{-1}, mean ± S.D., N=19 units) was higher than that of afferents that innervate Vnp canal neuromasts (x=19.4±8.6 dB decade^{-1}, N=19 units) (one-way ANOVA, P<0.001). These values agree with the expected amplitude slopes of ~40 dB decade^{-1} for an acceleration
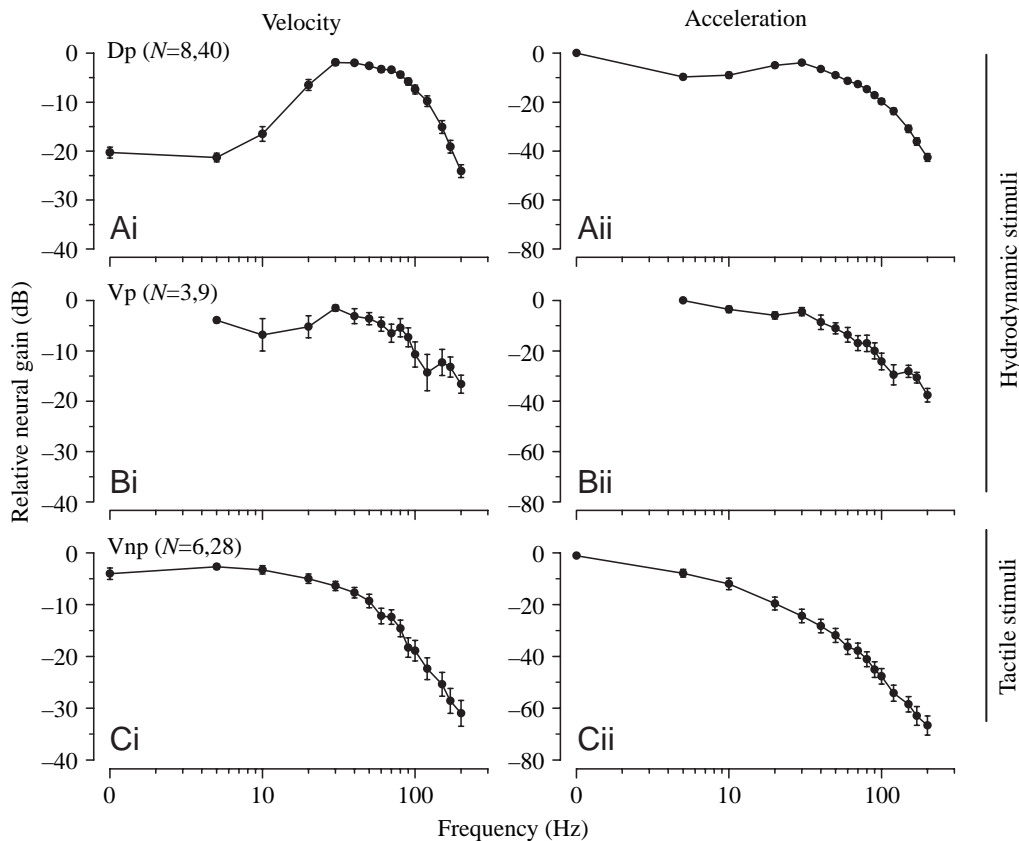

Fig. 6. Bode plots for frequency responses to hydrodynamic and tactile stimuli for primary afferent neurons that innervate lateral line canal neuromasts in the dorsal pored (Dp), ventral pored (Vp) and ventral non-pored (Vnp) hyomandibular canals of the Atlantic stingray, *Dasyatis sabina*. Hydrodynamic stimuli: Dp primary afferents show peak frequency sensitivity at 20–90 Hz re: velocity (Ai) and a flat, relatively untuned response up to about 40 Hz when expressed in terms of acceleration (Aii). Vp primary afferents show flat to low-pass characteristics when expressed in terms of both velocity (Bi; <70 Hz) and acceleration (Bii; <30 Hz). Variation among units is likely due to low sample size for this group (N=9). Tactile stimuli: Vnp primary afferents stimulated by tactile depression of the skin show a relatively flat response up to 30 Hz re: velocity (Ci) and a low-pass response re: acceleration (Cii) with a 6 dB drop in neural response achieved by 5 Hz. Thus, primary afferents from pored canals respond to hydrodynamic acceleration and units from ventral non-pored canals respond to the velocity of canal fluid induced by skin depression. Data were normalized to a relative value of 0 dB assigned to the best frequency for each neuron and expressed as relative neural gain (dB). All data are plotted as mean ± S.E.M. for each stimulus frequency relative to velocity (Ai–Ci) and acceleration (Aii–Cii). Sample sizes (N) represent the number of animals, number of primary afferents sampled. Note that some error bars are obscured by symbols.

detector and ~20 dB decade^{-1} for a velocity detector (Kroese et al., 1978), respectively. The low frequency slopes of afferents from Vp canal neuromasts (x=19.8±4.8 dB decade^{-1}, mean ± S.D., N=3 units) were similar to those from Vnp units, but the low sample size precludes conclusions from these data.

Phase relationships of the peak neural response relative to peak sphere displacement confirm these different sensitivities to velocity and acceleration (Fig. 7). Many afferents from Dp canal neuromasts showed a phase lead of approximately 180° at low frequencies (<20 Hz), while afferents from Vnp canals had a phase lead near 90° at low frequencies (<20 Hz) (Fig. 7). Phase increases at higher frequencies are at least partially due to differential primary afferent conduction times between the various stimulus and recording sites. Phase relationships of afferents from Vp canals were not analyzed, due to small sample size and high variation among units.

Primary afferent BF also differed among canal subsystems (Table 2; Fig. 8). Best frequency of acceleration-sensitive Dp primary afferents ranged from 1–40 Hz (x=21.7±1.7 Hz, mean ± S.E.M.), but the mode was at 30 Hz (Fig. 8). In contrast, while the range of BF for Vnp velocity sensitive afferents was also

Table 2. *Best frequency of lateral line primary afferent neurons that innervate neuromasts in the dorsal pored (Dp), ventral pored (Vp) and ventral non-pored (Vnp) hyomandibular canals of the stingray relative to displacement, velocity and acceleration*

	Dp (8, 40)	Vp (3, 9)	Vnp (6, 28)
Displacement	70, 80, 100	50, 80, 127.5	40, 50, 80
Mean ± S.E.M.	84.5±4.3	85.6±14.8	60.7±4.9
Velocity	30, 30, 40	30, 40, 65	5, 7.5, 10
Mean ± S.E.M.	34.5±2.5	48.9±7.9	8.6±1.3
Acceleration	10, 20, 30	5, 20, 30	1, 3, 10
Mean ± S.E.M.	21.7±1.7	18.3±4.3	5.5±1.2

Best frequencies (Hz) for units in each category were not normally distributed, thus statistics are expressed as 25%, median, 75% quartiles and mean ± S.E.M. The total number of animals, total number afferents sampled from each canal subsystem are indicated in parentheses.
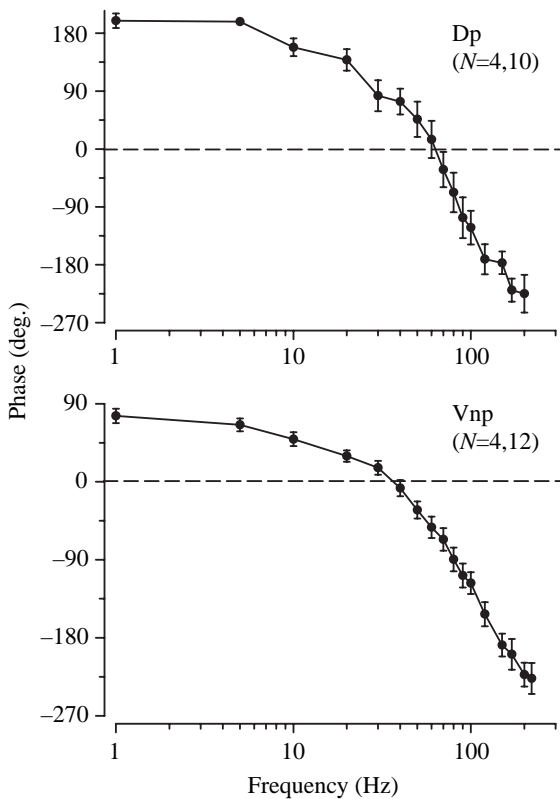

Fig. 7. Phase diagrams for frequency responses of primary afferent neurons from dorsal pored (Dp) and ventral non-pored (Vnp) hyomandibular canals in the Atlantic stingray, *Dasyatis sabina*. Dp primary afferents show a low frequency phase lead of about 180° (acceleration-sensitive), while Vnp primary afferents show a low frequency phase lead of about 90° (velocity-sensitive). Phase of the peak neural response is expressed in degrees (mean ± S.E.M.) relative to the peak displacement of the sphere. Sample sizes (N) show the number of animals, number of primary afferents analyzed.
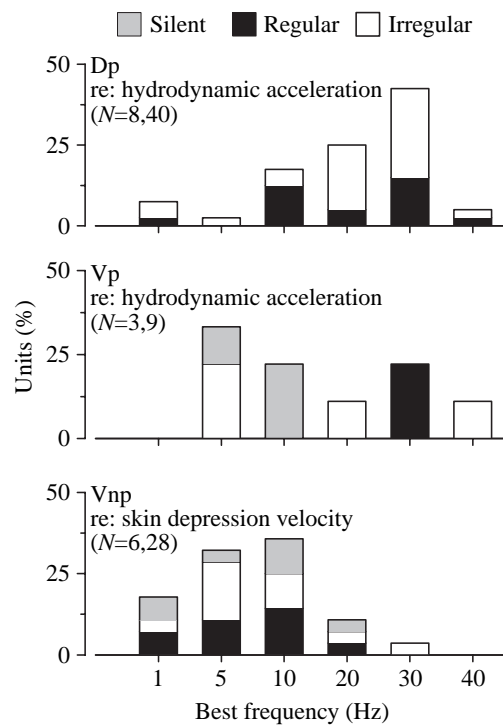

Fig. 8. Best frequency histograms of regular, irregular and silent primary afferent neurons from dorsal pored (Dp), ventral pored (Vp) and ventral non-pored (Vnp) hyomandibular canals in the Atlantic stingray, *Dasyatis sabina*. Best frequencies for primary afferents that innervate neuromasts in Dp and Vp canals are expressed re: hydrodynamic acceleration while those that innervate neuromasts in Vnp canals are expressed re: skin depression velocity. Primary afferents from Vnp canals respond best to low frequency velocity stimuli at ~5–10 Hz, while afferents from Dp canals respond best to acceleration stimuli at ~30 Hz. Vp canals responded to acceleration stimuli from 5–40 Hz, with the greatest percentage of units at 5 Hz. Silent, regular and irregular discharging primary afferents had similar best frequencies within each canal type. Sample sizes (N) show the number of animals, number of primary afferents sampled.

broad (1–30 Hz, x=8.6±1.3 Hz, mean ± S.E.M.), maximum BF mode was lower at 10 Hz (Fig. 8). Best frequency of the total population of afferents from Dp canals was higher than that of Vnp canals when all fiber responses were tested within a single category of displacement, velocity or acceleration (Kruskal–Wallis one-way ANOVA on ranks, Dunn's test, P<0.05). However, BF of the total population of afferents from Vp canals was higher than that of Vnp canals when tested within a single category of velocity or acceleration (Kruskal–Wallis one-way ANOVA on ranks, Dunn's test, P<0.05), but not displacement (Kruskal–Wallis one-way ANOVA on ranks, Dunn's test, P>0.05). Thus, in the context of biologically significant stimuli for these canal subsystems (velocity and acceleration), the population of afferents from pored canals were more sensitive to higher stimulus frequencies than those in non-pored canals. There was no difference in neural sensitivity (gain) at BF among canal subsystems in terms of velocity or acceleration (Kruskal–Wallis one-way ANOVA on ranks, Dunn's test, P>0.05; Table 3). The relationship between neural discharge and hydrodynamic acceleration for three individual Dp primary afferents shows that neural discharge increases as a function of stimulus intensity (Fig. 5). The most sensitive primary afferent in this example (0.31 spikes s^{-1}/mm s^{-2}) had a more than fourfold greater average peak discharge slope than the least sensitive afferent (0.07 spikes s^{-1}/mm s^{-2}). Mean neural sensitivity at best frequency ranged from 0.01 to 1.2 spikes s^{-1}/mm s^{-2} for Dp, 0.04 to 1.4 spikes s^{-1} per mm s^{-2} for Vp, and 5 to 86 spikes s^{-1}/mm s^{-2} for Vnp canals (Table 3).

Mechanotactile sensitivity

The prediction that non-pored canals should have a greater sensitivity to tactile stimuli than to hydrodynamic stimuli was supported. Afferents from Vnp canals showed phasic responses to skin depression velocities of approximately 30–630 μm s^{-1} from 1–20 Hz, and velocities as low as 63 μm s^{-1} to >5 mm s^{-1} at a frequency of 10 Hz. Primary afferents that innervate neuromasts in the non-pored ventral hyomandibular canal respond to direct tactile stimulation as well as to hydrodynamic

flow several mm above the canal. However, afferents were an average of 2–10 times more sensitive to tactile stimulation than to water movements directly above the tactile stimulus location (Fig. 9). This difference is most prominent at lower frequencies (10–20 Hz) where the mean change in neural sensitivity between tactile and hydrodynamic stimuli was 6.3±0.92 spikes s^{-1}/mm s^{-2} at 20 Hz (mean ± S.E.M.).

The tactile receptive field was also determined for 26 primary afferents that innervate neuromasts in the non-pored ventral hyomandibular canal. Receptive fields on the skin above the non-pored canals ranged from 0.25–4.0 cm^2 with a mean of 1.4±0.3 cm^2 (mean ± S.E.M.). Thus, rays are sensitive to tactile stimulation at least 2.5 mm lateral to the main canal on either side, which encompasses the size of benthic invertebrate prey (~2–10 mm) found in their diet.

Hair cell orientations

The prediction that non-pored canal neuromasts have a higher proportion of hair cells oriented off the longitudinal canal axis compared to hair cells on neuromasts within pored canals was not supported by SEM analyses. The majority of hair cells were oriented within 45° of the longitudinal canal axis in Dp (94%), Vp (93%) and Vnp (86%) canals (Fig. 10). These orientations indicate that about 90% of hair cells in all canals will respond with at least 70% (cos45°) of the maximum response to fluid flow along the longitudinal canal axis. Although there was no difference in hair cell orientations
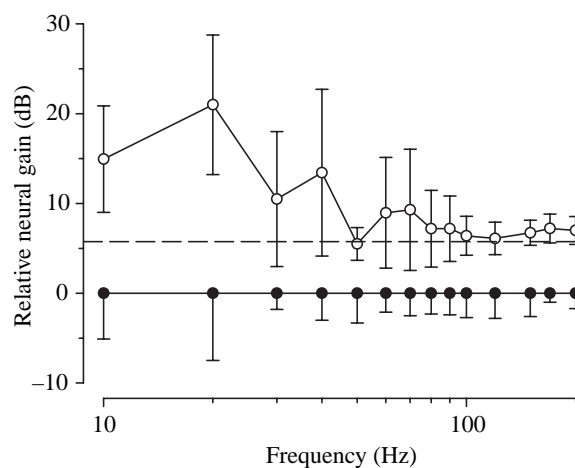
Fig. 9. Increase in relative neural gain to tactile stimulation over hydrodynamic flow for primary afferent neurons in the ventral non-pored hyomandibular canal of the stingray, *Dasyatis sabina*. Mean tactile sensitivity of three primary afferents from ventral non-pored canals (open circles) normalized relative to their average response to hydrodynamic flow above the canal (solid circles at 0 dB) across different stimulus frequencies are shown. Note that the average neural response is 6–20 dB greater to direct tactile stimuli compared to hydrodynamic stimuli above the canal, and are highest at the lower frequencies (10–20 Hz). Thus, non-pored canals are an average of 2–10 times more sensitive to tactile stimuli than to local water movements. Values are means ± S.E.M. and error bars are shown only in the negative direction on the 0 dB line for clarity. The broken line represents a relative neural gain of 6 dB.

Table 3. *Neural sensitivity at best frequency relative to velocity and acceleration for lateral line primary afferent neurons from dorsal pored (Dp), ventral pored (Vp) and ventral non-pored (Vnp) hyomandibular canals of the stingray*

	Dp (8, 40)	Vp (3, 9)	Vnp (6, 28)
Velocity (spikes s^{-1}/mm s^{-1})	34.2±6.8	37.3±10.0	33.0±5.0
Min, max	3, 89	7.5, 102	5, 86
Acceleration (spikes s^{-1}/mm s^{-2})	1.02±0.11	1.2±0.21	0.94±0.16
Min, max	0.01, 1.2	0.04, 1.4	0.04, 1.3

Values are means ± S.E.M. The total number of animals, total number of afferents sampled from each canal subsystem are indicated in parentheses. Min, minimum; max, maximum.
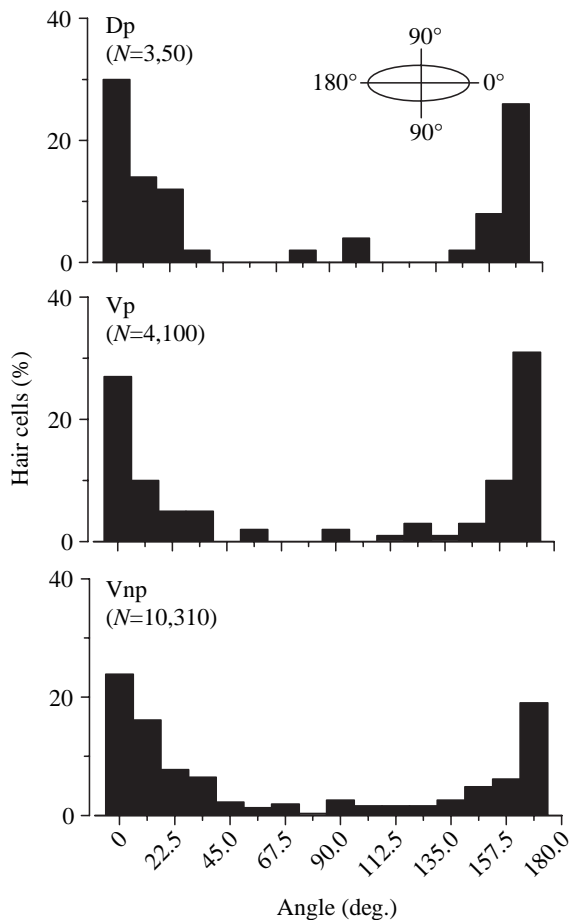
Fig. 10. Frequency distributions of hair cell orientations on lateral line canal neuromasts in the Atlantic stingray, *Dasyatis sabina*. The main neuromast and longitudinal canal axis lies along the 0–180° line (inset). Semicircular (from 0–180°) angular orientations from the canal axis are expressed as the percentage of total hair cells and compiled in 11.25° bins. Neuromasts in all three canal subsystems have the majority (>85%) of hair cells oriented within 45° of the main canal axis, and a small percentage oriented nearly orthogonal (90°) to this axis. However, there are no differences in hair cell orientations among dorsal pored (Dp), ventral pored (Vp) and ventral non-pored (Vnp) neuromasts. Sample sizes (N) represent the number of animals, number of hair cells measured.

among Dp, Vp and Vnp canal neuromasts (Kruskal–Wallis one-way ANOVA on ranks, $P=0.285$), about 6–14% of all hair cells were oriented within 45° of the orthogonal canal axis. Thus only a small percentage of hair cells would be most sensitive to localized lateral depressions of the canal wall.

Discussion

This study provides physiological evidence for a functional distinction between the stingray pored and non-pored lateral line canal subsystems. Our results show that primary afferents from pored canals on the dorsal and ventral surface have higher resting discharge activity and best frequencies than afferents from non-pored ventral canals. In addition, afferents from pored canals show properties consistent with acceleration detectors (i.e. they encode the fluid velocity in the canal driven by the acceleration or pressure gradient outside the canal) while responses of afferents from non-pored canals were proportional to the velocity of skin movements. These findings and the demonstration that the non-pored canals are more sensitive to tactile stimulation than to water movement stimuli provide neurophysiological support for the mechanotactile hypothesis of lateral line function.

Resting discharge activity

Lateral line primary afferents that lack any resting discharge (silent units) were encountered ~3–10 times more frequently in Vnp canals compared to Vp or Dp canals. Silent units in the lateral line of the cichlid fish were relatively insensitive to sinusoidal stimuli and were sometimes localized to injured neuromasts (Münz, 1985). This is not the case in the stingray because all silent units had sensitivities within the range of spontaneously active neurons. Silent afferents that discharge only in response to stimulation may be advantageous in the non-pored ventral canals of the stingray that encode transient movements of underlying skin caused by stimuli such as small excavated prey. Thus, this physiological subpopulation may serve as a discriminator of localized skin movements.

Spontaneous discharge activities of primary afferent neurons in the stingray are similar to those reported for lateral line systems in other fishes (Roberts, 1972; Münz, 1985; Tricas and Highstein, 1991; Kroese and Schellart, 1992). Interspike interval distributions within each class (regular and irregular) were variable, similar to those seen in lateral line afferents of the cichlid and other teleosts, and may be a function of fiber diameter and different conduction velocities (Münz, 1985). Primary afferents that innervate Dp canal neuromasts had higher resting discharge activity and shorter interspike intervals than afferents from Vnp canal neuromasts. Primary afferents that innervate canal neuromasts in most teleosts have higher discharge rates than those from superficial neuromasts, which is suggested to be a function of the increased size and greater hair cell to afferent convergence ratio of canal neuromasts (Münz, 1985, 1989). This contradicts results from the present study because primary afferents from Vnp canals of the stingray have a slower discharge rate, but innervate larger neuromasts and have a greater hair cell to afferent ratio than those in the Dp canal, which has afferents with a faster discharge rate (Maruska and Tricas, 1998; Lowrance, 2000). Thus, the difference in spontaneous discharge activity between Dp and Vnp canals cannot be explained by variations in convergence ratios, but rather, discharge regularity may be due to postsynaptic mechanisms, as suggested for the vestibular system (Goldberg et al., 1984; Boyle and Highstein, 1990).

Detection of lateral line stimuli requires central nervous system recognition of a change in primary afferent resting discharge rate or pattern. Afferents with fast regular discharge rates would show enhanced temporal resolution for encoding external stimuli, especially at low frequencies, due to the low

endogenous variance in resting interspike intervals. In contrast, irregular discharging units would better encode higher frequency information. Moving objects generally produce complex water motions, which may contain both high and low frequency components (Bleckmann et al., 1991). Thus, the mix of fiber types in all canal locations of the stingray can allow detection of a range of different frequencies potentially available to the lateral line system. Regular and irregular primary afferents within each canal subsystem differed in discharge variability (CV), but had similar best frequencies. Thus the functionality of regular *versus* irregular discharge patterns at the primary afferent level is unclear, but may be more important in central processing.

Frequency–response

Frequency–response characteristics of primary afferents indicate that pored canal systems function as acceleration detectors. Neural responses to sinusoidal stimulation at frequencies below best frequency increase in relative neural gain at a rate of 37 dB decade^{-1} and have a phase lead of about 180°, a typical response feature for an acceleration detector (Kroese and Schellart, 1992). Historically, frequency–response properties of lateral line primary afferent neurons are interpreted in terms of displacement of the stimulus source (see Kalmijn, 1989). However, canal neuromasts are known to be sensitive to water acceleration such that the flow velocity inside the canal is proportional to the net acceleration between the fish and surrounding water (for reviews, see Kalmijn, 1989; Coombs and Janssen, 1990b; Coombs and Montgomery, 1999) and there must be a pressure gradient across the canal pores to generate fluid flow inside the canal. Therefore, when frequency–response data are plotted in terms of acceleration, they exhibit broader tuning curves with relatively constant gain up to ~40–50 Hz and low-pass characteristics (BF<30 Hz) (Coombs and Janssen, 1989; Kalmijn, 1989). This is also true for the frequency–responses recorded from the stingray, which is consistent with those observed in teleosts and further illustrates the behavioral importance of low frequency velocity and acceleration information to the lateral line system.

The neural response of primary afferents to water motion is influenced by the morphologies of the canal, neuromast and cupula (Denton and Gray, 1988, 1989; van Netten and Kroese, 1989a,b). The lateral line canal system of elasmobranchs contains a main canal with a nearly continuous sensory epithelium and lateral neuromast-free tubules that terminate in pores on the skin (see Fig. 1). The frequency–response properties of lateral line primary afferents in the pored canals of the stingray are similar to those reported for teleosts in which only a single neuromast is found between two adjacent pores (Münz, 1985; Coombs and Janssen, 1990a; Kroese and Schellart, 1992). Thus, differences in neuromast, canal and pore organizations between bony and cartilaginous fishes are not reflected in overall response properties of primary afferent neurons. A comparable example in a single species exists in the Antarctic fish, *Trematomus bernacchii*, which has large variations in peripheral canal morphology but relatively

homogeneous frequency response properties (Coombs and Montgomery, 1992). In the stingray dorsal hyomandibular canal system, the increase in the number of pores associated with a single lateral tubule increases the receptive field area on the distal pectoral fins, similar to that observed for the prickleback, *Xiphister atropurpureus* (Bleckmann and Münz, 1990). These branched tubules on the dorsal surface indicate an increased sensitivity to water motions, possibly at a loss of spatial resolution, but the physiology data from the present study shows no difference in neural sensitivity among canal types. Thus, any functional significance of multiple neuromasts between adjacent pores or branched tubule patterns in elasmobranchs requires further investigation of parameters such as hair cell – afferent innervation; canal, neuromast and cupulae organization and mechanics; and projection patterns for central processing.

The dorsal hyomandibular canal in the Atlantic stingray is best positioned to detect water movements near the disk margin that may be generated by predators, conspecifics during social interactions, epifaunal or swimming prey items, and distortions in the animal's own flow field for object localization (Maruska, 2001). Such water movements are often transient and complex. Detection of the acceleration component of water motion by Dp canals is advantageous in that acceleration precedes the actual displacement of the object, thus resulting in an earlier response (Wubbels, 1992). The amplitude of acceleration is also relatively large at onset and offset of a movement, which would cause a strong response at the peripheral lateral line provided the stimulus is within the receptor bandwidth. Strong and quick responses at the periphery are essential for lateral line-mediated behaviors such as prey capture and predator detection in all aquatic species. Recordings from the brain of the batoid *Platyrhinoidis triseriata* show that fast transient events (high acceleration) best stimulate midbrain and forebrain lateral line regions (Bleckmann et al., 1989). Thus, the ability of the peripheral and central lateral line system to detect and encode transient acceleration stimuli supports its hypothesized biological functions in the stingray.

In contrast to pored canal systems, the response properties of primary afferents from non-pored canals of the stingray are not interpreted in terms of hydrodynamic stimuli. Neuromasts are enclosed within the canal and internal fluid motion is created by movement of the skin rather than by pressure gradients across skin pores. Frequency–response properties of afferents in non-pored canals show a low-frequency roll-off of 19 dB decade^{-1} and phase lead of about 90° to tactile stimulation, which is within the expected range for a velocity detector (Kroese and Schellart, 1992). However, because the hydrodynamic force acting on the cupula contains both a viscous and an inertial component, a fluid or boundary layer occurs around the cupula that ultimately influences the mechanical coupling of water and the neuromast (van Netten, 1991). The morphology of pored canals creates a high-pass filter that attenuates low frequencies (Denton and Gray, 1988). In contrast, the underlying compliant skin of non-pored canals may function as a low-pass filter that reduces high frequency

stimulation due to the physical constraints of skin movement. However, the mechanics of tissue distortion produced by tactile or hydrodynamic flow are likely complex and dependent on a number of factors such as the mechanical properties of the skin and canal. Variations in frequency–response properties between canal and superficial neuromasts of teleosts result from factors such as different stiffness coupling between cupula and hair cells, cupular geometry and canal dimensions (Denton and Gray, 1988, 1989; van Netten and Kroese, 1989; van Netten and Khanna, 1994). Thus, these characteristics may also contribute to the response differences observed in the pored and non-pored canals of the stingray and warrant further investigation.

The Atlantic stingray feeds almost exclusively on small benthic invertebrates, which they excavate from the sand substrate and contain in a feeding depression beneath the body (Cook, 1994; Bradley, 1996; Maruska and Tricas, 1998). Motile as well as sedentary animals can produce hydrodynamic flows and potential stimuli near the best frequency of the stingray lateral line canal system. For example, many zooplankton generate swimming vibrations of 5–50 Hz at constant swimming speeds of 10–15 cm s^{-1} (Montgomery, 1989), and bivalves generate hydrodynamic flow velocities of 6–14 cm s^{-1} (Price and Schiebe, 1978; LaBarbera, 1981). These values translate to accelerations in the cm s^{-2} range, which are well within the range of sensitivities seen at the primary afferent level in the stingray. Hydrodynamic flow fields generated by excavated prey can be detected by the pored section of the ventral hyomandibular canal and the stingray can move its body to position the non-pored canals, snout and, finally, the mouth directly above the prey for localization and final capture. Several meso- to bathypelagic fishes (e.g. *Anoplogaster* spp.) also have canal systems covered by thin, soft membranes without any regular system of pores. Studies indicate this morphology increases low-frequency sensitivity of the system and similar to the stingray, may facilitate foraging on small fishes, squid and crustaceans in low light environments (Denton and Gray, 1988).

Mechanotactile sensitivity

The mechanotactile hypothesis of lateral line function states that ventral non-pored canals function as tactile receptors to facilitate prey localization and capture (Maruska and Tricas, 1998). The present study confirms the prediction that primary afferents in the non-pored ventral canals respond as velocity detectors driven by movement of the skin. These afferents have receptive fields of 0.25–4 cm^2 on the skin surface, which is equivalent to or greater than the surface area of their small prey. Previous studies show that elasmobranch cutaneous tactile receptors respond to skin depressions of 20 μm (Murray, 1961), which is equivalent to a velocity of 1256 μm s^{-1} at 10 Hz. The present study shows that primary afferents from non-pored canals respond to skin motion velocities as low as 63 μm s^{-1} at 10 Hz. Thus the mechanotactile lateral line system appears to provide a twentyfold or greater sensitivity to tactile velocity stimuli and could increase the stingray's foraging efficiency on small benthic prey.

In order to assess possible advantages of Vnp canals for prey detection, we compared frequency responses to hydrodynamic and tactile stimuli among Vnp and Dp canal units, but because of time constraints were unable to compare responses to tactile stimuli between Vnp and Vp units. Without this control we can only assert that the non-pored lateral line system is specialized for tactile stimulation compared to pored canals. However, in addition to enhanced tactile sensitivity to prey, there may be other advantages for a non-pored lateral line system, which include the following: (1) Hydrodynamic stimuli from emergent and infaunal invertebrates (e.g. amphipods, polychaetes, echinoderms) are minimal or do not adequately stimulate the pored canal system. (2) Non-pored canals do not vent local lateral line fluid motion, thus they could enhance sensitivity to tactile stimuli along a greater length of the canal. This would be dependent upon tactile stimulus velocities and pore separation. (3) Development of a non-pored lateral line increases sensitivity to velocity and low frequency stimuli. (4) A non-pored system reduces intrusion of sediments (e.g. sand) through skin pores that can interfere with hydrodynamic stimulation. (5) The absence of canal pores would reduce self-generated hydrodynamic noise during excavation and manipulation of prey. This could result in an enhanced signal-to-noise ratio in primary afferent neurons.

Only a few studies examine the physiology of the lateral line in elasmobranchs, especially with regard to biological function of the system. Sand (1937) demonstrated that a constant flow in the ventral non-pored hyomandibular canal of the skate, *Raja* spp., increased primary afferent discharges, and that touch of the skin was also an effective stimulus for the lateral line in those species. However, any natural tactile or hydrodynamic stimulus should only cause a transient low volume movement of canal fluid and therefore the supra-threshold constant flows used in those experiments were not biologically relevant stimuli. Recordings in the medial octavolateralis nucleus (primary lateral line processing center in the hindbrain) in the thornback ray show responses to peak-to-peak (PTP) displacements of 0.02 μm (Bleckmann et al., 1987, 1989), which is considerably lower than that observed for primary afferents in the present study. This discrepancy may be explained by several factors. First, the lowest stimulus amplitude used for frequency–response analyses in the present study was approximately 0.5 μm PTP at the skin surface, but many primary afferents in the stingray responded to displacements much lower than 0.5 μm (K.P.M., personal observation). Second, the increased sensitivity in the central nervous system results from high signal-to-noise ratios of principal cells in the hindbrain due to convergence of many primary afferents onto a single secondary cell (Montgomery, 1984; Bleckmann and Bullock, 1989; Tricas and New, 1998). In addition, behavioral detection thresholds of sensory stimuli are often much lower than neurophysiological thresholds due to summation and sensory integration. Thus, in its natural environment the stingray may respond to water movements at thresholds much lower than indicated by their primary afferent responses.

Hair cell orientations

Maximum sensitivity to fluid flow in canals results from the orientation of hair cells and their kinocilia parallel to the main canal axis. While canals of some chondrichthyan species show these axial hair cell orientations (Hama and Yamada, 1977; Peach and Rouse, 2000), others have proportions of hair cells oriented nearly perpendicular to the canal axis (Roberts, 1969; Roberts and Ryan, 1971; Ekstrom von Lubitz, 1981). The majority of hair cells (86–94%) within all stingray canals were oriented within 45° of the longitudinal canal axis. However, all neuromasts also showed some hair cells that were oriented perpendicular to the canal axis (6–14%), which may broaden the sensitivity to tactile stimulation of the skin adjacent to the canal. Nevertheless, we found no difference in hair cell orientations among Dp, Vp and Vnp canals. Thus these results did not support our prediction that non-pored canals have a greater proportion of orthogonally oriented hair cells compared to pored canals. One function of the non-pored canals may be to facilitate movement of the body so that prey is passed along the canal axis towards the mouth (Maruska and Tricas, 1998), so the most effective hair cell orientation would be parallel to the canal axis as observed. The mechanotactile mechanism of action for ventral non-pored canals is also supported by the 0.25–4 cm^2 receptive field, large canal diameter that covers a greater area of underlying skin surface, and more compliant dermal skin layers compared to dorsal canals (Maruska and Tricas, 1998; Maruska, 2001). Collectively, this morphological evidence is consistent with the function of tactile receptors for the ventral non-pored canals of batoids, but the performance consequences of non-axial hair cells in pored canals remains to be determined.

In summary, our results show that the pored hyomandibular canals on the dorsal surface of the stingray differ in terms of primary afferent-response properties from the non-pored hyomandibular canals on the ventral surface. Primary afferents from dorsal pored canals respond as hydrodynamic acceleration detectors of transient water disturbances that may be caused by predators, conspecifics or prey. Ventral non-pored canals are sensitive to small movements of the skin and primary afferents encode the velocity of fluid induced in the canal by these stimuli. These results support the main predictions of the mechanotactile hypothesis and demonstrate a physiological basis for lateral line-mediated prey detection in this and possibly other elasmobranch species.

List of symbols and abbreviations

a	acceleration
BF	best frequency
CV	coefficient of variation
d	estimated peak-to-peak or peak displacement at the skin surface
D	distance between the center of the sphere and the skin
DC	mean resting rate
Dp	dorsal pored
f	sphere vibration frequency
HYO	hyomandibular canal
ISI	interspike interval
m	slope
R	radius of the sphere
S	distance between the points of maximum neural excitation and no response
U	amplitude of sphere displacement
u	velocity
Vnp	ventral non-pored
Vp	ventral pored

References

Bleckmann, H. and Bullock, T. H. (1989). Central nervous physiology of the lateral line, with special reference to cartilaginous fishes. In *The Mechanosensory Lateral Line – Neurobiology and Evolution* (ed. S. Coombs, P. Görner and H. Münz), pp. 387-408. New York: Springer-Verlag.

Bleckmann, H. and Münz, H. (1990). Physiology of lateral-line mechanoreceptors in a teleost with highly branched, multiple lateral lines. *Brain Behav. Evol.* **35**, 240-250.

Bleckmann, H., Breithaupt, T., Blickhan, R. and Tautz, J. (1991). The time course and frequency content of hydrodynamic events caused by moving fish, frogs, and crustaceans. *J. Comp. Physiol. A* **168**, 749-757.

Bleckmann, H., Bullock, T. H. and Jorgensen, J. M. (1987). The lateral line mechanoreceptive mesencephalic, diencephalic, and telencephalic regions in the thornback ray, *Platyrhinoidis triseriata* (Elasmobranchii). *J. Comp. Physiol. A* **161**, 67-84.

Bleckmann, H., Weiss, O. and Bullock, T. H. (1989). Physiology of lateral line mechanoreceptive regions in the elasmobranch brain. *J. Comp. Physiol. A* **164**, 459-474.

Boord, R. L. and Campbell, C. B. G. (1977). Structural and functional organization of the lateral line system of sharks. *Amer. Zool.* **17**, 431-441.

Boyle, R. and Highstein, S. M. (1990). Resting discharge and response dynamics of horizontal semicircular canal afferents of the toadfish, *Opsanus tau. J. Neurosci.* **10**, 1557-1569.

Bradley, J. L. (1996). Prey energy content and selection, habitat use and daily ration of the Atlantic stingray, *Dasyatis sabina*. MS thesis, Florida Institute of Technology, USA.

Chu, Y. T. and Wen, M. C. (1979). *Monograph of Fishes of China: A Study of the Lateral-Line Canal System and that of Lorenzini Ampullae and Tubules of Elasmobranchiate Fishes of China.* Shanghai, China: Science and Technology Press.

Cook, D. A. (1994). Temporal patterns of food habits of the Atlantic stingray, *Dasyatis sabina* (LeSeur, 1824), from the Banana River Lagoon, Florida. MS thesis, Florida Institute of Technology, USA.

Coombs, S. and Janssen, J. (1989). Peripheral processing by the lateral line system of the mottled sculpin (*Cottus bairdi*). In *The Mechanosensory Lateral Line – Neurobiology and Evolution* (ed. S. Coombs, P. Görner and H. Münz), pp. 299-319. New York: Springer-Verlag.

Coombs, S. and Janssen, J. (1990a). Behavioral and neurophysiological

assessment of lateral line sensitivity in the mottled sculpin, *Cottus bairdi*. *J. Comp. Physiol. A* **167**, 557-567.

Coombs, S. and Janssen, J. (1990b). Water flow detection by the mechanosensory lateral line. In *Comparative Perception – Volume II: Complex Signals* (ed. C. Stebbins and M. A. Berkley), pp. 89-123. New York: Wiley and Sons, Inc.

Coombs, S. and Montgomery, J. C. (1992). Fibers innervating different parts of the lateral line system of the Antarctic fish, *Trematomus bernacchii,* have similar neural responses despite large variations in peripheral morphology. *Brain Behav. Evol.* **40**, 217-233.

Coombs, S. and Montgomery, J. C. (1999). The enigmatic lateral line system. In *Comparative Hearing: Fish and Amphibians* (ed. R. R. Fay and A. N. Popper), pp. 319-362. New York: Springer-Verlag.

Denton, E. J. and Gray, J. A. B. (1988). Mechanical factors in the excitation of the lateral line of fishes. In *Sensory Biology of Aquatic Animals* (ed. J. Atema, R. R. Fay, A. N. Popper and W. N. Tavolga), pp. 595-593. Berlin Heidelberg New York: Springer-Verlag.

Denton, E. J. and Gray, J. A. B. (1989). Some observations on the forces acting on neuromasts in fish lateral line canals. In *The Mechanosensory Lateral Line – Neurobiology and Evolution* (ed. S. Coombs, P. Görner and H. Münz), pp. 229-246. New York: Springer-Verlag.

Ekstrom von Lubitz, D. K. J. (1981). Ultrastructure of the lateral-line sense organs of the ratfish, *Chimaera monstrosa*. *Cell Tiss. Res.* **215**, 651-665.

Ewart, J. C. and Mitchell, H. C. (1892). On the lateral sense organs of elasmobranchs. II. The sensory canals of the common skate (*Raja batis*). *Trans. R. Soc. Edinburgh* **37**, 87-105.

Flock, A. (1965). Electron microscopic and electrophysiological studies on the lateral line canal organ. *Acta Otolaryngol.* **Suppl. S199**, 7-90.

Goldberg, J. M., Smith, C. E. and Fernandez, C. (1984). Relation between discharge regularity and responses to externally applied galvanic currents in vestibular nerve afferents of the squirrel monkey. *J. Neurophysiol.* **51**, 1236-1256.

Hama, K. and Yamada, Y. (1977). Fine structure of the ordinary lateral line organ II. The lateral line canal organ of the spotted shark, *Mustelus manazo*. *Cell Tiss. Res.* **176**, 23-36.

Johnson, S. E. (1917). Structure and development of the sense organs of the lateral canal system of selachians (*Mustelus canis* and *Squalus acanthias*). *J. Comp. Neurol.* **28**, 1-74.

Kalmijn, A. J. (1989). Functional evolution of lateral line and inner-ear sensory systems. In *The Mechanosensory Lateral Line – Neurobiology and Evolution* (ed. S. Coombs, P. Görner and H. Münz), pp. 187-215. New York: Springer-Verlag.

Kroese, A. B. A., Van der Zalm, J. M. and Van den Bercken, J. (1978). Frequency response of the lateral-line organ of *Xenopus laevis*. *Pflüg. Archiv.* **375**, 167-175.

Kroese, A. B. and Schellart, N. A. M. (1992). Velocity- and acceleration-sensitive units in the trunk lateral line of the trout. *J. Neurophysiol.* **68**, 2212-2221.

LaBarbera, M. (1981). Water flow patterns in and around three species of articulate brachiopods. *J. Exp. Mar. Biol. Ecol.* **55**, 185-206.

Lowrance, C. (2000). The development of the mechanosensory and electrosensory lateral line: a model of sensitivity and resolution. MS thesis, Florida Institute of Technology, USA.

Maruska, K. P. (2001). Morphology of the mechanosensory lateral line system in elasmobranch fishes: ecological and behavioral considerations. *Environ. Biol. Fish.* **60**, 47-75.

Maruska, K. P. and Tricas, T. C. (1998). Morphology of the mechanosensory lateral line system in the Atlantic stingray, *Dasyatis sabina*: the mechanotactile hypothesis. *J. Morph.* **238**, 1-22.

Montgomery, J. C. (1984). Frequency response characteristics of primary and secondary neurons in the electrosensory system of the thornback ray. *Comp. Biochem. Physiol.* **79A**, 189-195.

Montgomery, J. C. (1989). Lateral line detection of planktonic prey. In *The Mechanosensory Lateral Line – Neurobiology and Evolution* (ed. S. Coombs, P. Görner and H. Münz), pp. 561-574. New York: Springer-Verlag.

Montgomery, J. C. and Skipworth, E. (1997). Detection of weak water jets by the short-tailed stingray *Dasyatis brevicaudata* (Pisces: Dasyatidae). *Copeia* **1997**, 881-883.

Montgomery, J. C., Baker, C. F. and Carton, A. G. (1997). The lateral line can mediate rheotaxis in fish. *Nature* **389**, 960-963.

Münz, H. (1985). Single unit activity in the peripheral lateral line system of the cichlid fish *Sarotherodon niloticus* L. *J. Comp. Physiol. A* **157**, 555-568.

Münz, H. (1989). Functional organization of the lateral line periphery. In *The Mechanosensory Lateral Line – Neurobiology and Evolution* (ed. S. Coombs, P. Görner and H. Münz), pp. 285-297. New York: Springer-Verlag.

Murray, R. W. (1961). The initiation of cutaneous nerve impulses in elasmobranch fishes. *J. Physiol.* **159**, 546-570.

Peach, M. B. (2001). The dorso-lateral pit organs of the Port Jackson shark contribute sensory information for rheotaxis. *J. Fish Biol.* **59**, 696-704.

Peach, M. B. and Rouse, G. W. (2000). The morphology of the pit organs and lateral line canal neuromasts of *Mustelus antarcticus* (Chondrichthyes: Triakidae). *J. Mar. Biol. Assn UK* **80**, 155-162.

Price, R. E. and Schiebe, M. A. (1978). Measurements of velocity from excurrent siphons of freshwater clams. *Nautilus* **92**, 67-69.

Roberts, B. L. (1969). Mechanoreceptors and the behavior of elasmobranch fishes with special reference to the acoustico-lateralis system. In *Sensory Biology of Sharks, Skates, and Rays* (ed. E. S. Hodgson and R. W. Mathewson), pp. 331-390. Arlington, Virginia: Office/Naval Research.

Roberts, B. L. (1972). Activity of lateral-line organs in swimming dogfish. *J. Exp. Biol.* **56**, 105-118.

Roberts, B. L. and Ryan, K. P. (1971). The fine structure of the lateral-line sense organs of dogfish. *Proc. R. Soc. Lond. B* **179**, 157-169.

Sand, A. (1937). The mechanism of the lateral sense organs of fishes. *Proc. R. Soc. B* **123**, 472-495.

Späth, M. and Schweickert, W. (1977). The effect of metacaine (MS-222) on the activity of the efferent and afferent nerves in the teleost lateral-line system. *Naunyn-Schmiedebergs Arch. Pharmakol.* **297**, 9-16.

Tricas, T. C. and Highstein, S. M. (1991). Action of the octavolateralis efferent system upon the lateral line of free-swimming toadfish, *Opsanus tau*. *J. Comp. Physiol. A* **169**, 25-37.

Tricas, T. C. and New, J. G. (1998). Sensitivity and response dynamics of elasmobranch electrosensory primary afferent neurons to near threshold fields. *J. Comp. Physiol. A* **182**, 89-101.

van Netten, S. M. (1991). Hydrodynamics of the excitation of the cupula in the fish canal lateral line. *J. Acoust. Soc. Amer.* **89**, 310-319.

van Netten, S. M. and Khanna, S. M. (1994). Stiffness changes of the cupula associated with the mechanics of hair cells in the fish lateral line. *Proc. Nat. Acad. Sci.* **91**, 1549-1553.

van Netten, S. M. and Kroese, A. B. A. (1989a). Hair cell mechanics controls the dynamic behavior of the lateral line cupula. In *Cochlear Mechanisms: Structure, Function and Models* (ed. J. P. Wilson and D. T. Kemp), pp. 47-55. New York: Plenum.

van Netten, S. M. and Kroese, A. B. A. (1989b). Dynamic behavior and micromechanical properties of the cupula. In *The Mechanosensory Lateral Line – Neurobiology and Evolution* (ed. S. Coombs, P. Görner and H. Münz), pp. 247-263. New York: Springer-Verlag.

Wubbels, R. J. (1992). Afferent response of a head canal neuromast of the ruff (*Acerina cernua*) lateral line. *Comp. Biochem. Physiol.* **102A**, 19-26.